# Continuum drift kinetic electron closures in NIMROD*

**Eric Held, J. Andrew Spencer, Jeong-Young Ji, Trevor Taylor, Brett Adair, Tyler Markham, Hankyu Lee, McKay Murphy the NIMROD Team, and Joseph Jepson, and Chris Hegna (U. Wisconsin-Madison)**

Department of Physics
**UtahState**University

**CTTS Meeting, April 3, 2022, Santa Rosa, CA**

*Work supported by DOE under grant nos. DE-FG02-04ER54746, and DE-SC0018146.

# Outline

- Improvements in NIMROD continuum kinetics v2.*.
- NIMROD prediction for Sauter coefficients in DIII-D IBS discharge #174446.
- NIMROD prediction for bootstrap current in DIII-D IBS discharge #174446.

# NIMROD continuum kinetics v2.0

- Improved parallelism over speed points:
  - reduced memory, speed groups only store their segment of distribution functions
  - mirrors NIMROD's decomposition over Fourier modes, DO im=1,nmodes -> DO is=1,ns num(species)
  - moments require communication between speed groups.
- Data and loop reordering significantly optimized continuum kinetic integrand routines:

| | **Collision Loop** | **Streaming Loop** | **Total Matrix-Vector** |
|---|---|---|---|
| before | 380 | 88 | 480 |
| after | 70 | 15 | 106 |

- Implementation of regularity condition, $\partial F/\partial\xi = 0$ at $s = 0$ for Gauss-Radau schemes: $\int_0^\infty dse^{-s^2}F = w_1F(s_1 = 0) + \sum_{n=2}^{ns} w_nF(s_n)$.

# NIMROD continuum kinetics v2.1

- Much improved accuracy and efficiency for field terms in linearized Coulomb collision operator (Spencer *et al., JCP*, **450** (2022) 110862).

$$\int_{-1}^{1} d\xi\, H_b(v,\xi)\, Q_l(\xi) = v^2 \int_0^{\infty} d\bar{v} \sum_{l'} F_{b,l'}(v\bar{v})\, \mathsf{K}_{ll'}(\bar{v}) \tag{8}$$

$$\int_{-1}^{1} d\xi\, \frac{\partial H_b}{\partial v}(v,\xi)\, Q_l(\xi) = v \int_0^{\infty} d\bar{v} \sum_{l'} F_{b,l'}(v\bar{v}) \left[\mathsf{Kp}_{ll'}(\bar{v}) - \frac{1}{2}\mathsf{K}_{ll'}(\bar{v})\right] \tag{9}$$

$$\int_{-1}^{1} d\xi\, \frac{\partial^2 G_b}{\partial v^2}(v,\xi)\, Q_l(\xi) = v^2 \int_0^{\infty} d\bar{v} \sum_{l'} F_{b,l'}(v\bar{v}) \left[\mathsf{Epp}_{ll'}(\bar{v}) - \frac{1}{4}\mathsf{E}_{ll'}(\bar{v})\right] \tag{10}$$

where the precomputed kernels are

$$\mathsf{E}_{ll'}(\bar{v}) \equiv \int_{-1}^{1} d\xi \int_{-1}^{1} d\xi'\, Q_l(\xi)\, Q_{l'}(\xi')\, \bar{v}^{5/2} \int_0^{2\pi} d\gamma' \left(v^{-1}\bar{v}^{-1/2}u\right) \tag{11}$$

- Significantly speeds up kernel calculations ($K_{ll'}, E_{ll'}, ...$) when using high-order, trapped/passing FE basis functions, $Q_l(\xi)$.

# NIMROD continuum kinetics v2.2

- Fully implicit implementation of moment terms in CEL-DKE, J. R. Jepson, *et al.*, Phys. Plasmas **28**, 082503 (2021).
- Ion stress tensor in ion CEL-DKE a good example:

$$\pi_{\|} = p_{\|} - p_{\perp} = = 2\pi m (\frac{2T}{m})^{5/2} \int_0^\infty ds s^4 \int_{-1}^{1} d\xi (\frac{3}{2}\xi^2 - \frac{1}{2}) F$$

- Need moments of $\Delta F = F^{k+1} - F^k$ for time-implicit treatment of

$$\Delta F - \Delta t \frac{v'_{\|}}{nT} \mathbf{b} \cdot [\frac{2}{3} \nabla \pi_{\|}(\Delta F) - \pi_{\|}(\Delta F) \nabla \ln B] = ....$$

  Accuracy is significantly improved with mass matrix inversion to project iterate onto NIMROD's 2D FE representation.
- For more details on ion CEL-DKE in NIMROD:
  14. Joseph Jepson - University of Wisconsin - Madison - Simulations of plasma flow evolution of an axisymmetric tokamak using a Chapman-Enskog-like (CEL) kinetic closure approach in NIMROD
  Monday, 4 April 2022, 1:30PM-3:30PM

# NIMROD continuum kinetics v2.3

- Pitch-angle ($\xi$) FE grids with nodes at local trapped/passing boundary critical for keeping velocity dofs reasonable.

J.A. Spencer, B. Adair, E.D. Held et al. Journal of Computational Physics 450 (2022) 110862

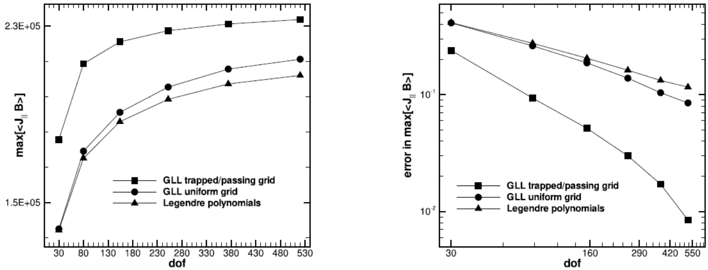


**Fig. 14.** The maximum of $< J_{||} B >$ from Fig. 13 (left) is plotted against degrees of freedom ($dof$) for the *tpb* GLL FE grids, uniform GLL FE grids and the Legendre basis. The error of each (right) is measured against a case using $(N_s, N_\xi) = (19, 58)$. The computational savings offered by *tpb* GLL FE grids is significant in these 4-D calculations.

# NIMROD continuum kinetics v2.4

- Electron and ion delta-f and CEL-DKE integrand routines combined to reduce code volume and compilation time.
- Simple time-centering scheme shows promise:
  $(\mathbf{V}, F_e)^k \quad (n, \mathbf{B}, T_e, T_i, F_i)^{k+1/2} \quad (\mathbf{V}, F_e)^{k+1}$
  Diagonal-in-s preconditioning matrices for DKE's updated about every 20-50 timesteps with dt=2.e8. DKE time comparable to fluid time.
- To do list
  - Experiment with more sophisticated, simultaneous implicit advances
    $(\mathbf{V}, F_i)^k \quad (n, \mathbf{B}, T_e, T_i, F_e)^{k+1/2} \quad (\mathbf{V}, F_i)^{k+1}$
    For more details see 14. Andrew Spencer - Utah State University - Time advance schemes for continuum drift kinetics and extended MHD, Monday, 4 April 2022, 1:00PM-6:00PM
  - Implement fully nonlinear, non-relativistic Coulomb collision operator following on successful implementation of relativisitc version.
    5. Tyler Markham - Utah State University - Relativistic, Continuum Drift-Kinetic Capability in the NIMROD Plasma Fluid Code, Monday, 4 April 2022, 4:00PM-6:00PM
  - Reduce memory highpoint during factorization of diagonal-in-s preconditioning matrices.

# Need tight fluid/kinetic coupling for bulk species.

- Relatively easy $\delta f$ applications include:
  - solving for electron and ion $\delta f$'s to predict neoclassical transport in axisymmetric toroidal geometry
  - advancing energetic particle $\delta f$ and coupling to MHD through closure for anisotropic pressure tensor.

- Numerical formulation relatively easy since thermodynamic drives have a simpler form.

- Allows for easy testing of needed velocity space resolution and significance of *ad hoc* terms like an effective diffusion: $D\nabla^2 F$ in DKE.

- Simplified delta-f computations are a useful prelude to long time scale, self-consistent hybrid fluid/kinetic simulations with CEL-DKE closures.

# Piggyback on successful NIMROD NTM simulation.

- Start from equilibrium used in [Howell et al., Phys. Plasmas 2022],
- Keep everything the same but replace heuristic neoclassical electron stress and diffusive parallel heat flow closure with electron CEL-DKE closures.

The heuristic force resulting from the neoclassical ion stress is modeled as

$$\nabla \cdot \vec{\vec{\pi}}_i = \mu_i n m_i \left\langle B_{eq}^2 \right\rangle \frac{(\vec{v} - \vec{v}_{eq}) \cdot \vec{e}_\Theta}{\left(\vec{B}_{eq} \cdot \vec{e}_\Theta\right)^2} \vec{e}_\Theta, \qquad (8)$$

and the heuristic force resulting from the neoclassical electron stress is [14]

$$\nabla \cdot \vec{\vec{\pi}}_e = -\mu_e \frac{m_e}{e} \left\langle B_{eq}^2 \right\rangle \frac{\left(\vec{J} - \vec{J}_{eq}\right) \cdot \vec{e}_\Theta}{\left(\vec{B}_{eq} \cdot \vec{e}_\Theta\right)^2} \vec{e}_\Theta. \qquad (9)$$

| | Simulation | Experiment |
|---|---|---|
| Lundquist Number | $2.5 \times 10^6$ | $7.9 \times 10^6$ |
| Prandtl Number | 23 | 11 |
| $(\chi_\parallel/\chi_\perp)^{1/4}$ | 100 | 260 |
| $\mu_e$ | $8 \times 10^5 [s^{-1}]$ | $1.3 \times 10^5 [s^{-1}]$ |
| $\mu_i$ | $1 \times 10^3 [s^{-1}]$ | $1.4 \times 10^3 [s^{-1}]$ |
| $\mu_e/(\nu_{ei} + \mu_e)$ | 0.55 | 0.43 |

Table I: Simulation parameters evaluated at the 2/1 surface, and experimental parameters for comparison.

# Robust 2/1 NTM growth kicked off by an ELM.

- ELM triggers NTM in DIII-D IBS discharge #174446 at 3396 ms.
- NIMROD seeds the NTM using an external magnetic perturbation imposed on equilibrium reconstruction at 3390 ms.

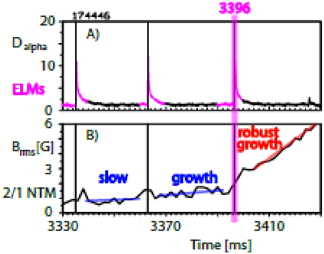


Figure 2: Experimental time traces of the $D_{alpha}$ signal, and $n = 1$ $B_{rms}$ for the DIII-D reference discharge used in this study. An ELM at 3396 ms excites a robustly growing 2/1 NTM. Simulations use kinetic reconstruction of conditions at 3390 ms.

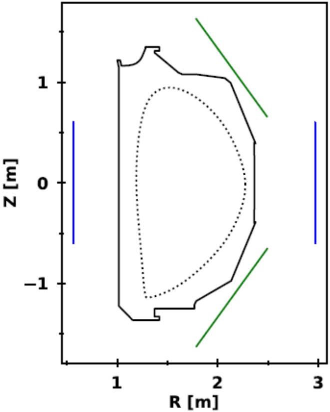

# Close fluid moments equations.

- In the Ramos theory(Ramos, *Phys Plasmas* **17**, 082502 (2010)), low-order fluid-moment evolution written as

$$\frac{\partial n}{\partial t} + \nabla \cdot n\mathbf{u} = 0$$

$$mn(\frac{\partial \mathbf{u}}{\partial t} + \mathbf{u} \cdot \nabla \mathbf{u}) - qn(\mathbf{E} + \mathbf{u} \times \mathbf{B}) + \nabla(nT) + \nabla \cdot [\pi_{\|}(\mathbf{bb} - \mathbf{I}/3)] - \mathbf{F}^{\mathrm{coll}} = 0$$

$$\begin{aligned} \frac{3n}{2}\frac{dT}{dt} + nT\nabla \cdot \mathbf{u} + \nabla \cdot (q_{\|}\mathbf{b} + \frac{5nT}{2qB}\mathbf{b} \times \nabla T) - G^{\mathrm{coll}} \\ -\pi_{\|}[\frac{1}{3}\nabla \cdot \mathbf{u} - \mathbf{bb} \cdot \nabla \mathbf{u}] = 0 \end{aligned}$$

# Use Chapman-Enskog-like (CEL) DKE for bulk species.

- Assume $f = f_{\mathrm{M}} + f_{\mathrm{NM}}$ with $\bar{f}_{\mathrm{NMe}} = O(\delta^2 f_{\mathrm{Me}})$ and $\bar{f}_{\mathrm{NMi}} = O(\delta f_{\mathrm{Mi}})$.
- Write CEL-DKE in the fluid frame (Ramos, *Phys Plasmas* **17**, 082502 (2010)):

$$\frac{\partial \bar{f}_{\mathrm{NM}}}{\partial t} + v'_{\parallel}\mathbf{b}\cdot\nabla\bar{f}_{\mathrm{NM}} - \frac{1-\xi^2}{2\xi}v'_{\parallel}\mathbf{b}\cdot\nabla\ln B\frac{\partial\bar{f}_{\mathrm{NM}}}{\partial\xi}$$
$$+\frac{v_0}{2}(\mathbf{b}\cdot\nabla\ln n)[\xi\frac{\partial\bar{f}_{\mathrm{NM}}}{\partial s} + \frac{1-\xi^2}{s}\frac{\partial\bar{f}_{\mathrm{NM}}}{\partial\xi}] - s[\xi\mathbf{b}\cdot\nabla + \frac{\partial}{\partial t}]\ln v_0\frac{\partial\bar{f}_{\mathrm{NM}}}{\partial s} = \langle C(f)\rangle$$
$$+\Bigg[(\frac{5}{2} - s^2)v'_{\parallel}\mathbf{b}\cdot\nabla\ln T + \frac{v'_{\parallel}}{nT}\mathbf{b}\cdot[\frac{2}{3}\nabla\pi_{\parallel} - \pi_{\parallel}\nabla\ln B - \mathbf{F}^{\mathrm{coll}}]$$
$$+2s^2(\frac{3}{2}\xi^2 - \frac{1}{2})[\frac{1}{3}\nabla\cdot\mathbf{u} - \mathbf{bb}\cdot\nabla\mathbf{u}] + \frac{2}{3nT}(s^2 - \frac{5}{2})[\mathbf{b}\cdot\nabla q_{\parallel} - q_{\parallel}\mathbf{b}\cdot\nabla\ln B - G^{\mathrm{coll}}]$$
$$+\frac{2}{3eB}s^2(\frac{3}{2}\xi^2 - \frac{1}{2})[(\frac{5}{2} - s^2)(\nabla\ln B - 2\kappa) + \nabla\ln n]\cdot\nabla T\times\mathbf{b}$$
$$+\frac{4}{3eB}(\frac{s^4}{2} - \frac{5}{2}s^2 + \frac{15}{8})(\nabla\ln B + \kappa)\cdot\nabla T\times\mathbf{b}\Bigg]f_M$$

# Definition of closure moments.

- Desired closure moments computed using random velocity:

$$
\begin{aligned}
\pi_\parallel = p_\parallel - p_\perp &= \frac{m}{2}\int d\mathbf{v}\big(3[\mathbf{b}\cdot(\mathbf{v}-\mathbf{u})]^2 - |\mathbf{v}-\mathbf{u}|^2\big)\bar{f}_{\mathrm{NM}} \\
&= 2\pi m(\frac{2T}{m})^{5/2}\int_0^\infty ds s^4 \int_{-1}^1 d\xi(\frac{3}{2}\xi^2 - \frac{1}{2})\bar{f}_{\mathrm{NM}} \\
q_\parallel &= \frac{m}{2}\int d\mathbf{v}\big([\mathbf{b}\cdot(\mathbf{v}-\mathbf{u})]|\mathbf{v}-\mathbf{u}|^2\big)\bar{f}_{\mathrm{NM}} \\
&= \frac{8\pi T^3}{m^2}\int_0^\infty ds s^5 \int_{-1}^1 d\xi \xi \bar{f}_{\mathrm{NM}} \\
\mathbf{F}_e^{\mathrm{coll}}/(n_e e) &= (m_e/n_e e)\int d\mathbf{v}(\mathbf{v}-\mathbf{u})C_{\mathrm{ei}}[f_e, f_i] \\
&= \eta_\perp \mathbf{J} - \frac{3}{2}\frac{n_e}{B}\eta_\perp \mathbf{b}\times\nabla T_e - \frac{6\pi^{3/2}e}{m_e^2}T_e^2\eta_\perp \int_0^\infty ds \int_{-1}^1 d\xi \xi \bar{f}_{\mathrm{NM}}\mathbf{b} \\
G_e^{\mathrm{coll}} &= \frac{m_e}{2}\int d\mathbf{v}|\mathbf{v}-\mathbf{u}|^2 C_{\mathrm{ei}}[f_e, f_i] \approx \frac{3e^2 n_e^2 \eta_\perp}{m_i}(T_i - T_e)
\end{aligned}
$$

# Back to NTM case. $T_e$ and $n_e$ from pfile.

- Howell *et al.* use $p_i = p_{total} - n_e T_e$ and quasineutrality with $Z_{eff} = 1$ to specify $n_i$ and $T_i$.

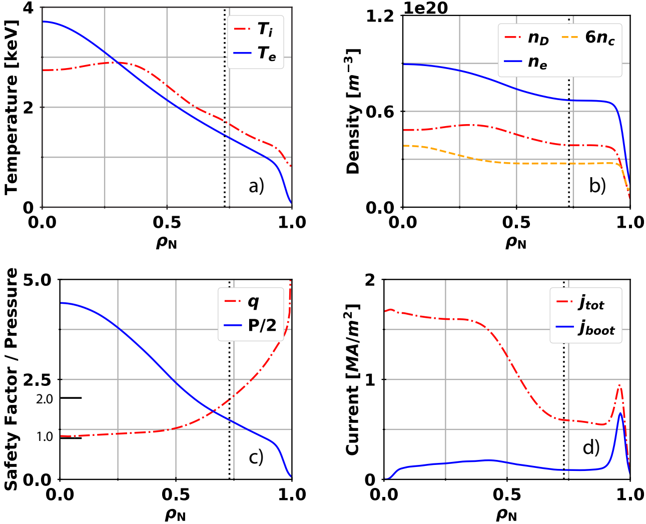

# Sauter-coefficients-benchmark as a test case.

- Necessary velocity space resolution can be quickly tested by computing Sauter coefficients using NIMROD continuum kinetics:

$$x\xi \frac{\partial f_{e1}^{(p)}}{\partial \theta} - \frac{(1-\xi^2)x}{2\hat{B}} \left( \frac{\partial \hat{B}}{\partial \theta} \right) \frac{\partial f_{e1}^{(p)}}{\partial \xi} - \frac{\nu'}{qR_0 \boldsymbol{b} \cdot \nabla \theta} \hat{C} = \frac{1+\xi^2}{2} x^2 e^{-x^2} \frac{1}{\hat{B}^2} \frac{\partial \hat{B}}{\partial \theta}$$

$$\mathcal{L}_{31} = -4\pi^{-1/2} \left\langle \hat{B} \int_{-1}^{1} d\xi \int_0^\infty dx \; x^3 \xi f_{e1}^{(p)} \right\rangle$$

$$\mathcal{L}_{32} = -4\pi^{-1/2} \left\langle \hat{B} \int_{-1}^{1} d\xi \int_0^\infty dx \; x^3 \xi f_{e1}^{(T_e)} \right\rangle$$

# Published results of Sauter-coefficients-benchmark.

- From Spencer *et al.*, *JCP*, **450** (2022) 110862:

J.A. Spencer, B. Adair, E.D. Held et al. Journal of Computational Physics 450 (2022) 110862

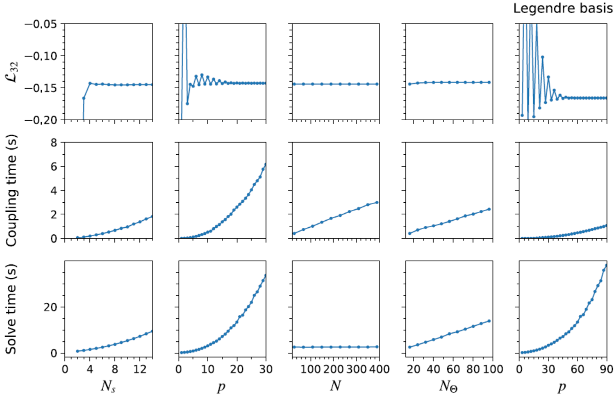


**Fig. 18.** Bootstrap current coefficient $\mathcal{L}_{32}$ and wall-clock timing with respect to numerical parameters: $N_s$ speed collocation points, $p$ polynomial degree for the *tpb* GLL FE basis, $N$ maximum number of Legendre polynomials used in far-field expansion, and $N_\Theta$ FE cells in poloidal angle. For comparison, the right-most column shows the results using the Legendre basis scanning in $p = 3, 6, \cdots, 87, 90$. Except for quantities being scanned, the base numerical parameters are $N_s = 6$, $p = 9$, $N = 29$, $N_\Theta = 16$. The first three parameters, $N_s$, $p$, and $N$, control the other parameters discussed in Algorithm 1. In every case, $N_\psi = 4$, bi-quadratic finite elements are used to discretize the annulus in the poloidal plane, and rather than scanning $N_{\bar{v}3}$ separately, $N_{\bar{v}3} = N_{\bar{v}1}$.

# 2D FE spatial grid and *tpb* velocity grid in core.

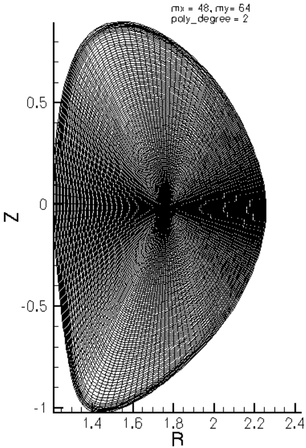


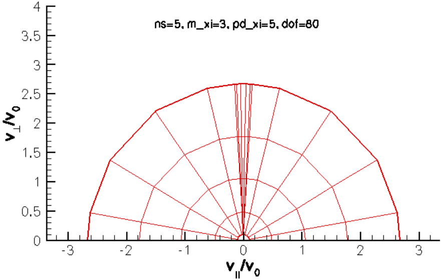

# 2D FE spatial grid and *tpb* velocity grid at edge.

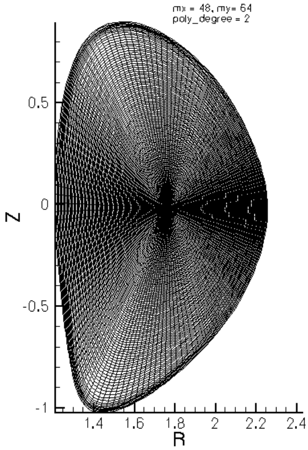


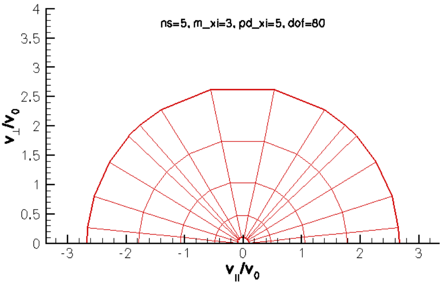

# Comparison of *tpb* velocity grids at edge.

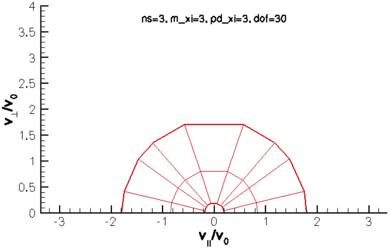


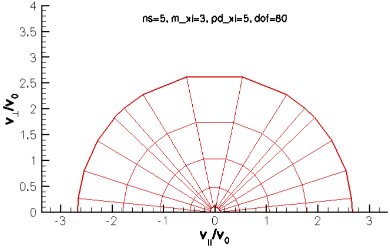


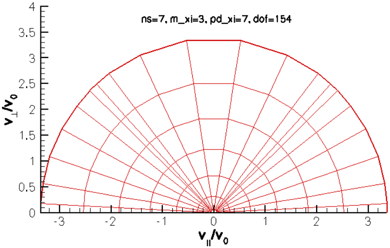

# Rapid convergence in Sauter coefficients.

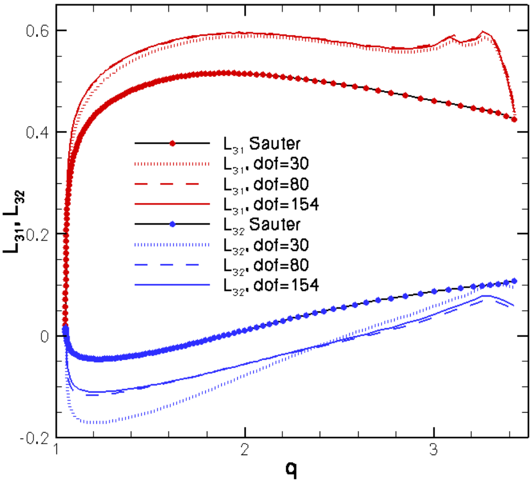

# Verification of equilibrium bootstrap current.

- NIMROD's calculation of equilibrium bootstrap current agrees with prediction in iterdb file. Velocity grid: ns=4, pd xi=4, dof=42.

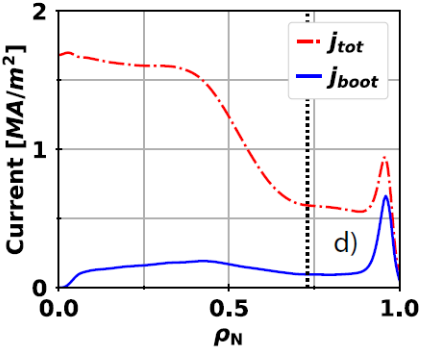


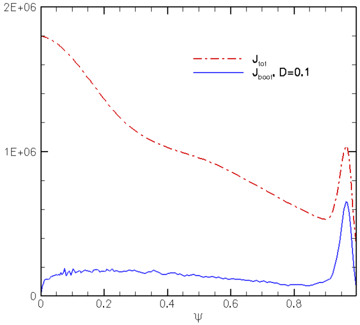

# Bootstrap response sensitive to artificial diffusion in DKE.

- Need $D\nabla^2 F$ for spatial smoothing in DKE, but be careful that it isn't too large.

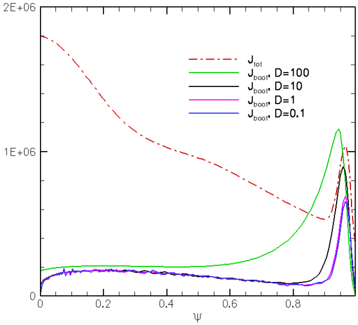


- Sauter coefficient and bootstrap current calculations help to quickly determine input parameters for continuum kinetics coupled to NIMROD's fluid model for NTM simulations.

# Future Work.

- Evolve electron CEL-DKE to steady state in axisymmetric geometry.
- Evolve coupled electron CEL-DKE/NIMROD-fluid system to steady state in axisymmetric geometry.
- Apply external magnetic perturbation and compare response from kinetic and heuristic viscous stress closures.
- Carry out NTM simulation with electron CEL-DKE closures.